Long Time Evolution of Unstable Bichromatic Waves

J.H. Westhuis*[†], E. van Groesen*, R. Huijsmans[†]

1 Introduction

The instability of wave trains has been a topic of research since [1] showed that the traveling wave solution of the non-linear water wave problem is unstable to modulational perturbations of its envelope. Many authors have studied these instabilities and confirmed the B-F instability growth-rates. When [7] showed that the Benjamin-Feir instability is also produced by the Nonlinear-Schrödinger (NLS) equation of weakly nonlinear wave theory, the long term behavior of the initial instability has been sought in terms of desintegration of the modulated wavetrain into solitary wave envelopes [2, 3].

For applications in hydrodynamic laboratories, the evolution and the resulting maximal wave heights are of practical interest. An experimental study by [4] in which the spatial evolution of a bichromatic wave group envelope is reported, motivated the research of this presentation. We numerically investigate with a nonlinear potential time domain method the long time evolution and spatial distribution of unstable bichromatic wavegroups and observe (in most cases) a recurrence phenomena. For moderate cases a 'simple' periodicty in the spatial evolution of the spectrum may be observed. However, with increasing initial amplitudes, more complicated (periodic) structures may be observed. Our current work aims at classifying these phenomena and find experimentally relations between characteristic quantities. In the final section we derive a stability criterion and a partial theoretical explanation of the phenomena.

2 Numerical method

The fluid is considered two dimensional, incompressible, inviscid and irrotational, which allows the velocity field to be defined by a potential function. The dynamic and kinematic boundary conditions on the free surface are integrated in time using a 5 step, 4th order Runge-Kutta scheme. Evaluating the right hand side of these equations involves the solution of Laplace's equation on the interior of the fluid. This solution is obtained using a linear Finite Element Method on a grid that is refined near the free surface. An artificial beach is constructed using a combination of pressure damping, grid stretching and Sommerfeld conditions tuned at the critical wavespeed $\sqrt{gh}$; the damping properties are remarkably good [6].

At the generating side of the domain, we used three different kind of generators to exclude that the observed effects are related to the specific way of wave generation. i) Moving flap: a moving hinged flap , ii) Linearized flap: the fluxes of the real flap are generated on a static vertical wall iii) Linear solution; the flux generated at the fixed vertical wall is derived from the expression for linear water waves. Although the signals differ from each other (which is to be expected), this difference consists of relatively small phase differences, the characteristic deformation of the wavegroup envelope is still observed (Fig. 1) and power spectra are almost identical. For further calculations we used the linearized flap, because it is easier to perform stable computations than with the moving geometry and it is more similar to a physical wave tank than the imposed linear solution. From these observations regarding the beach and wave generation and from qualitative comparisson of our numerical results with the experiments in [4], we conclude that the observed phenomena are only due to the nonlinearity of the equations and are not a consequence of numerical wave generation or absorbtion.

3 Phenomenon and simulations

We have conducted a series of numerical experiments for bichromatic waves with the two frequencies centered around 2s on a water depth of 5 meter. In all cases, both amplitudes are equal and denoted with q. The experimental model test results of [4] ($T_1 = 1.9s$, $T_2 = 2.1s$, $q = 0.08m$), and recent experiments at MARIN by Huijsmans & Westhuis 1999 , show strong asymmetric wave envelope deformation. The numerical simulations reproduce these findings; moreover: the computations have been extended to simulate a 1200 m wavetank (h=5m) wich uncovers dynamics which is not

*Department of Mathematical Sciences, University of Twente, The Netherlands

[†]Maritime Research Institute Netherlands (MARIN) Wageningen, The Netherlands.

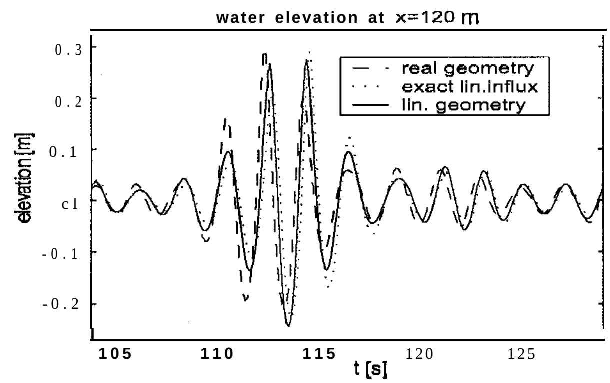

Figure 1: Comparison of the wave elevation of the unstable bichromatic wave generated by a moving hinged flap (dashed line), a hinged flap with linearized geometry (full line) and with the exact linear flux solution of the bichromatic wave prescribed (dotted line).

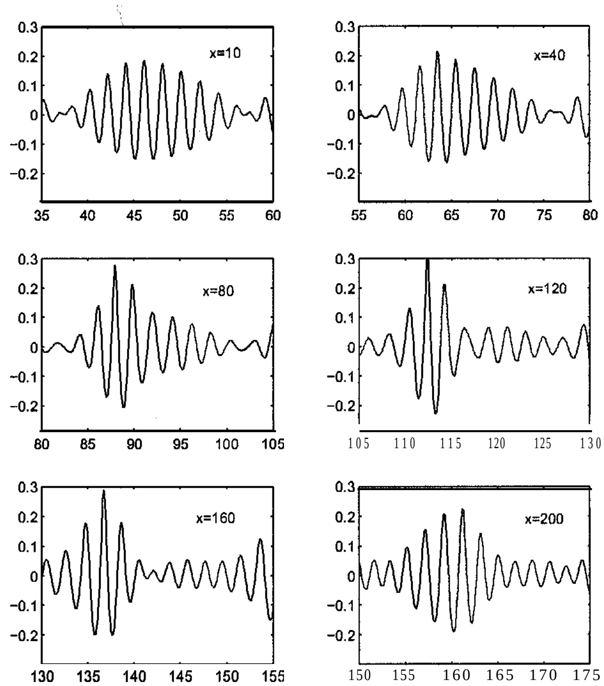

Figure 2: Time signals of a single wave group at different positions, 10, 40, 80, 120, 160, 200 m, from the wave maker, showing the asymmetrisation and increase of amplitude.

recognizable in physical laboratories. First we will describe the results for the model test mentioned above; then the evolution of the spectrum for different, cases will be compared.

For the model test case, according to linear theory, the modulated wave group would be described by $\eta(x, t) = 2q\cos(\Delta kx - \Delta\omega t)\cos(\bar{k}x - \bar{\omega}t)$ where $\bar{\omega} = \pi$, $\bar{k} \approx 1$ are the averaged frequency and wave number respectively, and Aw $\approx$ n/20 , $\Delta k \approx 0.1$ are half the differences. In the figures below, time signals at different positions of the tank show the unstable evolution characterised by large deformations of the envelope: the characteristic temporal beat pattern close to the wave maker is gradually deformed into more confined, much higher waves connected by smaller amplitude waves. For distances of the laboratory, this is shown in Fig. 2; for larger distances, Fig. 3 shows that the smaller waves form a second wave group that splits from the original one and merges with the successive larger group. On even larger distances, Fig. 4, it is seen that the splitting and merger process is a recurrent phenomenon. The temporal behaviour is periodic with period determined by the driving modulation period $\pi/\Delta\omega \approx 20$; the spatial recurrence takes place on an interval of approx. 400 m, much larger than the spatial periodicity of the linear solution which is $\pi/\Delta k \approx 10\ \pi$.

Now we consider the change in the spectrum of the bi-chromatic waves; and compare the above model test with other cases that have different values of the frequency difference or amplitude. In situations where the initial frequencies are well seperated $(T_1, T_2) = (1.8, 2.2)$ no spatial variations have been observed. For smaller frequency differences, such as in figure 5 for $(T_1, T_2) = (1.9, 2.1)$, the spectrum changes with increasing distance from the wavemaker, with periodic growth and decay of several sideband modes. The first side band modes $(2\omega_1 - \omega_2, 2\omega_2 \quad \omega_1)$ are observed for larger amplitudes; for $q = 0.08$, even significant energies at the frequencies $3\omega_1 \quad 2\omega_2$ and $4\omega_1 - 3\omega_2$ are clearly visible. (Higher initial amplitudes led to breaking within 900 seconds.) For smaller frequency differences, the instability shows itself already for smaller amplitudes.

Examination of the results has shown that there is a correlation between the spatial periods (and growth rates) of the sideband modes and the period of the initial waves. It is remarkable to notice that also the side band frequencies that lay well out of the B-F instability intervals (situations with $q = 0.04$, $q = 0.06$) show significant, growth rates, which indicates that a different kind of analysis is needed when examining the instability of these wavegroups; this will be done next.

4 Theoretical description

It is possible to construct a simplified model to describe and partly explain the observed phenomena by analysing an NLS-type of envelope equation. To that aim, we write in lowest order $\eta(x, t) = a \exp i(K(\bar{\omega})x - \bar{\omega}t + \phi) + c.c.$ with real amplitue a, and phase $K(\bar{\omega})x -$

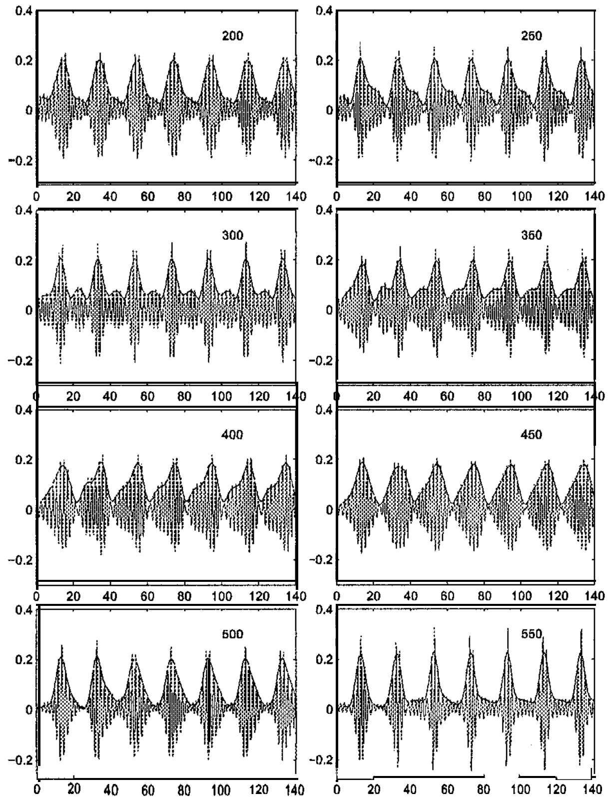

Figure 3: Time signals at larger distances (200 . 550 m) from the wave maker, showing the splitting and merger of a small wave group.

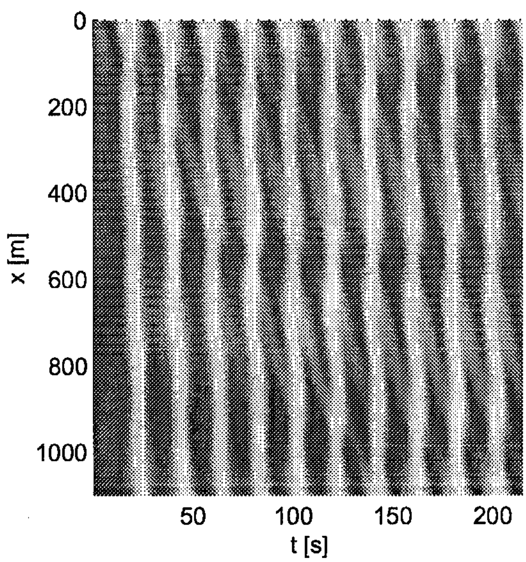

Figure 4: Density plot in a moving frame of reference, showing the splitting and merger of a small wave group.

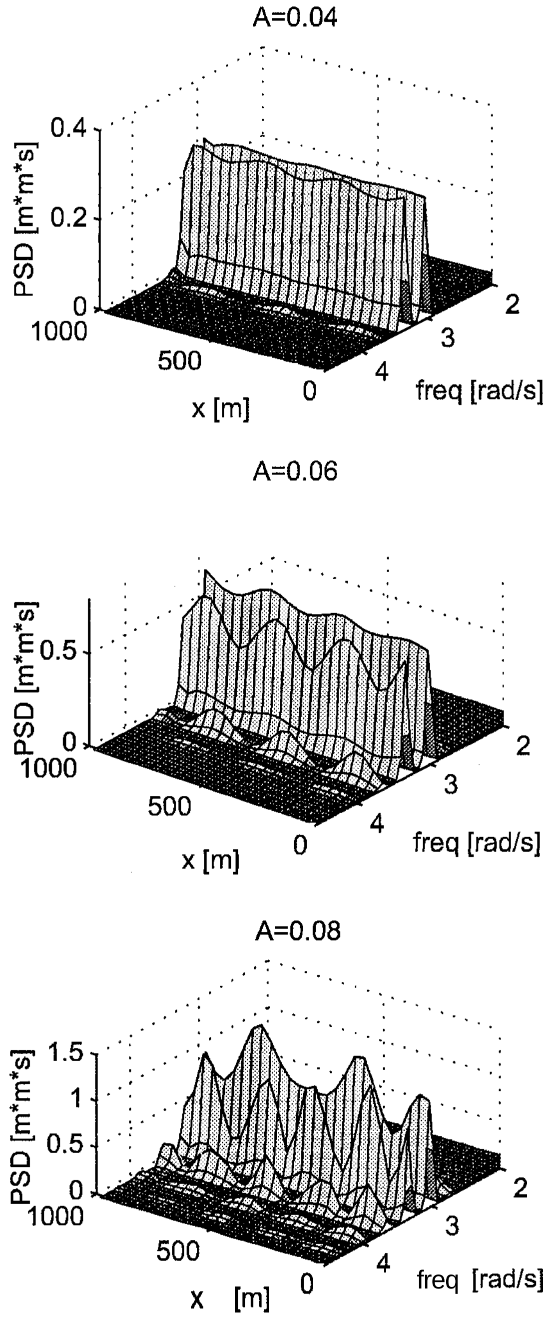

Figure 5: Spatial evolution of the spectrum of the bichromatic wave for different amplitudes. The periods of the bichromatic modes are $(T_1, T_2) = (1.9, 2.1)$ and the depth of the tank is 5 meters. Clearly the periodic structure of the nonlinear spatial evolution is visible for smaller amplitudes. However, for larger amplitudes this simple periodicity does no longer hold.

$\bar{\omega}t + \phi$, where $K(\bar{\omega})$ is the wave number corresponding to the avaraged frequency according to linear dispersion. Then the NLS equation contains certain parameters β (from group velocity dispersion) and γ (from nonlinear generation of second harmonic). The parameter β is positive, but, the sign of γ depends on the dispersive properties [5]. For applications in laboratories, with relatively short waves: a KdV-type of dispersion is not applicable and would lead to a negative value for γ (and diverging NLS). Instead, using the dispersion relation for small waves of any wave length: i.e. in normalised variables w = $\sqrt{k \tanh k}$, the coefficient γ is positive: self-focussing NLS, and the essential features are recovered. To illustrate this, it is simplest to work with the phase-amplitude equations. These can be written in various forms; in the following description, for direct interpretation, we use the physical frequency w and wavenumber lc, and the 'energy', or squared envelope, $E = a^2$. Then, using as variables $\tau = t - x/V_0$, $\xi = x$, with V_0 the central group velocity, energy and wave conservation, the phase equation, are given by, respectively,

$$\partial_\xi E + \partial_\tau [2\beta(\omega - \bar{\omega})E] = 0$$

$$\partial_\xi \omega + \partial_\tau [k - \tfrac{\omega}{V_0}] = 0, \quad K(\omega) - k = \gamma E + \beta \frac{\partial_\tau^2 a}{a}$$

The last equation is the non-linear dispersion relation (NDR), where the linear dispersion relation is modified with terms that account for a nonlinear correction, and a dispersive driven profile contribution (Yuen & Walker, Fornberg &Whitham).

For the signal problem for the bi-chromatic wave: at $\xi = 0$, the frequency is fixed w = $\bar{\omega}$, and the amplitude is the modulation $a = q\cos(\Delta\omega\tau)$. Then, the NDR produces the wave number as $k = \bar{k} - \gamma q^2 \cos^2(\Delta\omega\tau)$, after which the change in frequency is found for increasing ξ, and, consecutively, the change in energy. The result, is that, initially, in each modulation period, the frequency is skew-symmetric, and the envelope increases in the middle and decreases at the sides. This indicates that near $\xi = 0$, the cosine-profile changes into a sharper peaked pulse profile. With increasing distance, the profile further deforms.

A phenomenological investigation of possible instability can be based on the fact that the model with the correct dispersion is the self-focussing NLS equation and initial data on the whole real line will develop into solitons and residual radiation. For a soliton to exist it is necessary that the quantity K(w) $- k$ is positive. The restriction to periodic (temporal) intervals then restricts the possibility for such a soliton to develop in the following way. The energy per period generated at the wave maker is proportional to $q^2/\Delta\omega$. Any NLS-soliton has width inversely proportional to its amplitude, which itself is proportional to its energy. By the temporal periodicity of the observed phenomena, this means that, the soliton amplitude and energy should at least be proportional to Aw. Comparing the generated energy and that of a soliton implies that the quotient $q/\Delta\omega$ should exceed a critical value to explain the appearance of at least one large amplitude soliton within each temporal period, providing a stability criterion that resembles the condition for Benjamin-Feir modulational instability of a uniform wave train.

5 Conclusions

Detailed and accurate numerical simulations of wave forms, their envelopes and spectra of unstable wave-groups were presented on very long spatial and time intervals. It was found that for an initially bi-chromatic wave, instability arises when the wave height or the inverse frequency difference is sufficiently large. The instability was shown to be noticable in transfer of energy to sideband modes in a quasi periodic manner; taking the spatial structure per mode to be periodic, an experimental dependence between the spatial wavenumber and the wavenumber of the principal mode was found. Theoretically, an instability condition was derived for this case; although it resembles somewhat the BF-instability condition for uniform wave trains, no direct relation has been found between the observed growth rates of side band modes and the standard BF-predictions. A possible explanation may be that the growth rates in the bi-chromatic instability are determined by the enforced periodicity of the envelope and are a manifestation of the development of the confined soliton-type shapes within that period.

References

[1] T. Benjamin and J. Feir. The desintegration of wave trains in deep water. part 1. theory. *J. Fluid Mech.*, 27:417, 1967.

[2] V. Chu and C. Mei. The nonlinear evolution of stokes waves in deep water. *J. Fluid Mech.*, 47:337, 1971.

[3] H. Hasimoto and H. Ono. Nonlinear modulation of gravity waves. *J. Phys. Soc. Japan*, 33:805, 1972.

[4] C. Stansberg. On the nonlinear behavior of ocean wave groups. *proc. Waves '97*, 2:1227–1241, 1997.

[5] E. Van Groesen. Wave groups in uni-directional surface wave models. *J. Eng. Math.*, 34:215–226, 1998.

[6] J. Westhuis. A numerical beach for two and three dimensional fullt nonlinear numerical wave tanks. In *Proc. of the 10th ISOPE* conference, 2000. submitted.

[7] H. Yuen and B. Lake. Nonlinear deep water waves: theory and experiment. *Phys. Fluids*, 18:956, 1975.